On the Dye-Protein Interaction of TMR-Biocytin – Streptavidin Complex: Molecular Simulations and Time-Resolved Fluorescence Quenching

Jang Mok Yoo,[a] *Sujin Lee,*[b] *Hahkjoon Kim,**[b] *and Young Min Rhee**[a]

[a] Department of Chemistry, Korea Advanced Institute of Science and Technology (KAIST), Daejeon 34141, Korea

[b] Department of Chemistry, College of Science and Technology, Duksung Women's University, Seoul 01369, Korea

*E-mail: khj730516@duksung.ac.kr

*E-mail: ymrhee@kaist.ac.kr

Abstract

The interaction of a fluorophore and a protein, as a type of chemical-protein interactions (CPIs), is important toward studying physical properties of a protein through spectroscopy. For example, the structural changes of a protein can often be followed with spectroscopic tools by utilizing such an interaction. Streptavidin-bound 5-(and-6)-tetramethylrhodamine (TMR) biocytin is one of the few systems with which CPI can actually be observed via the fluorescence of TMR. While it has been suggested that the fluorescence is quenched when the ligand is bound to the binding pocket of streptavidin and is recovered after biotin occupies the binding pocket to replace TMR, no clear evidence has been provided yet. In order to gain a better understanding of this CPI, here we propose a possible binding site of TMR in the streptavidin, and predict the binding affinity values of biotin and the TMR moiety of TMR-biocytin conjugate. We estimate that the biotin affinity (−20.2 ± 1.4 kcal/mol) is significantly higher than the TMR-biocytin affinity (−6.91 ± 0.72 kcal/mol and −8.06 ± 0.79 kcal/mol), which supports the earlier explanation on the fluorescence quenching and recovery of biotinylated dyes. We also discover that TMR cannot bind to the streptavidin pocket as perfectly as biotin does, but that it rather blocks the entrance portion of the binding pocket. Fluorescence quenching of TMR-biocytin by streptavidin is measured with time-resolved fluorescence to show that the average fluorescence lifetime of TMR-biocytin decreases from 3.54 ns to 2.54 ns in the presence of excess streptavidin. Based on the distance between TMR and the nearby tryptophan residues, we propose that the nearby tryptophan residues of streptavidin are the potential quenchers of the dye unit fluorescence.

Introduction

Streptavidin is a tetrameric protein purified from the bacterium *Streptomyces avidinii* with a molecular weight of 52.4 kDa. It has a very high affinity for biotin with a dissociation constant

(K_d) of ~10^{-14} mol/L, and the combined pair displays one of the strongest non-covalent interactions known in nature. For this reason, it is widely used in biotechnology fields such as biomolecule detection and pre-targeted immunotherapy.[1]

Biotin plays a considerable role in biochemical processes and metabolism such as fatty acid synthesis specifically in carboxylation reactions, which takes the biotin coenzyme as a carbon dioxide carrier.[2] It is known that biotin deficiency causes many adverse effects on the human body, such as dermatosis, nausea, anorexia, and muscle pains.[3] Due to its importance, many techniques of measuring the biotin concentrations in samples have been reported.[4-6] A prominent technique employs biotinylated dyes with covalently attached fluorophore units to biotin to ensure that the fluorophore can be strongly associated with streptavidin.[7] Tetramethylrhodamine(TMR)-biocytin, a conjugate of biocytin and rhodamine fluorophore, is one such example of biotinylated dyes. Indeed, its strong binding with streptavidin has been adopted in various protein detection techniques[8] and molecular imaging methods.[9] When a biotinylated fluorophore binds to streptavidin, a change in fluorescence is usually observed. Gruber and coworkers reported that some biotinylated fluorophores exhibited fluorescence quenching when bound to streptavidin and that the fluorescence was recovered in the presence of sufficient biotin.[10] They were actually able to accurately measure the concentration of streptavidin by monitoring the quenching and the recovery of fluorescence. The "ostrich quenching model" has been proposed to account for the fluorescence quenching arising from the weak interaction of biotinylated dyes with streptavidin, with which the behavior of streptavidin and biotinylated dye is metaphorized to the ostrich's habit of hiding its head in the sand. Namely, the model explains that the fluorescence from the dye unit is quenched when it is bound to a nearby vacant binding pocket in addition to the more strongly binding biotinylating group. When more biotin is added to the system, the equilibrium of the dye-

streptavidin binding is shifted to release the dye unit, and its fluorescence is recovered. The majority of biotin assay techniques using biotinylated dyes apply this concept. Based on this, techniques to detect biotin impurities[11, 12] and to qualitatively measure the degree of reagent mixing[13, 14] were also proposed. In addition, it was predicted that there were two possibilities of quenching biotinylated dye fluorescence: one by the fluorophore/streptavidin interaction and the other by the fluorophore-fluorophore interaction.[15] While the former will prevail when less than three pockets are occupied at low enough concentration of the biotinylated dye, the latter will take place when most of the streptavidin pockets are occupied by them, usually in the 4:1 ratio with the streptavidin. In this latter case, the dangling dyes will have a high chance of approaching each other.

Even with the wide use of the TMR-biocytin for practical purposes, reports that characterize its fluorescence properties have been surprisingly scarce. On the experiment side, Osborne used the total internal reflection fluorescence dipole imaging to study the fluorescence emission from a single TMR-biocytin molecule bound to streptavidin attached to a biotinylated bovine serum albumin (BSA) on a glass coverslip.[16] He reported that the TMR dipole adopts a limited number of preferred orientations due to the interaction between the zwitterionic TMR probe and the charged residues on the streptavidin surface. On the theory side, to the best of our knowledge, there has been no study that explains the interaction between fluorophores and streptavidin, especially with enough details at the molecular level. Understanding the structure and dynamics around the binding event will be essential in figuring out the groups in the protein that specifically interact with the fluorophores and in elucidating the quenching mechanism of the dyes. In addition, it will be crucial toward gaining a better insight into the fluorophore-streptavidin interaction and potentially enhancing the accuracy of current biotin assay techniques. Furthermore,

it will allow us to access the fundamental aspects of weak chemical-protein interactions (CPIs). In fact, CPI is one of the paramount topics in the field of biochemistry, as it plays a crucial role in many fundamental biological processes such as metabolism. Thus, analyzing CPIs can help developing drugs as well as interpreting many biochemical cycles. Because experimentally determining CPIs is sometimes very challenging, theoretical means can often provide invaluable information. In this regard, a system composed of streptavidin, biotin, and biotinylated dyes can be considered as one of the very few systems where CPIs can be thoroughly monitored.

Here, we adopt TMR-biocytin and streptavidin as a model system for analyzing weak CPI. We propose plausible binding structures of 5- and 6-TMR-biocytin molecules (Fig. 1) using the molecular docking technique and predict the associated binding free energies by subsequently employing the umbrella sampling method[17-19] in combination with molecular dynamics (MD) simulations. The use of biasing potentials along a reaction coordinate not only enhances the sampling on the system but also guides toward valuable information about the important regions along the coordinateand the energy landscape of the system. We compare the calculated binding affinity values of TMR-biocytin with that of biotin and confirm that biotin indeed plays a major role in recovering the TMR fluorescence. We also show that there exists a weak interaction between TMR itself and streptavidin. Then we observe the time-resolved fluorescence quenching/recovery of biotinylated TMR, and propose a new mechanism for the photophysical phenomenon based on the predicted structures and binding affinities.

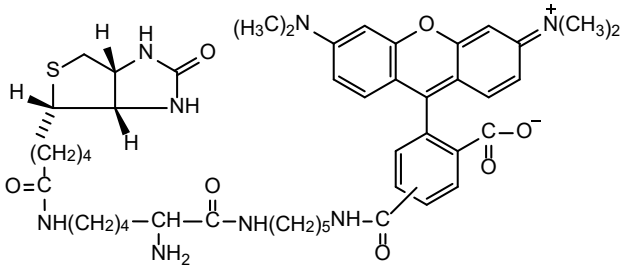

Fig. 1 Chemical structure of 5-(and-6)-tetramethylrhodamine-biocytin.

Materials and Methods

Simulation: system preparation

The starting configuration of streptavidin and the binding site of biotin were fetched from Protein Data Bank (PDB entry : 1STP).[20] Biotinylated TMRs were modeled by using Avogadro[21, 22] and their geometries were optimized with the universal force field (UFF)[23]. The docking structures of the ligands were proposed by Autodock Vina[24]. The program provided 20 models, some of which were practically identical (Table S1 in Supporting Materials). Among these, the one with the highest affinity and with the biotin part bound to monomer **1** was selected (Fig. 2). To confirm the consistency, we have performed docking simulations five times for each case. In addition, the convergence was examined by changing various parameters, such as exhaustiveness and the size of the search space. All selected structures for each docking simulation did not show any significant difference. Interestingly, the proposed docking structure (Fig. 2) clearly illustrated that TMR cannot bind to the receptor pocket as perfectly as biotin. Rather, the TMR group blocked the entrance portal of the biotin binding pocket.

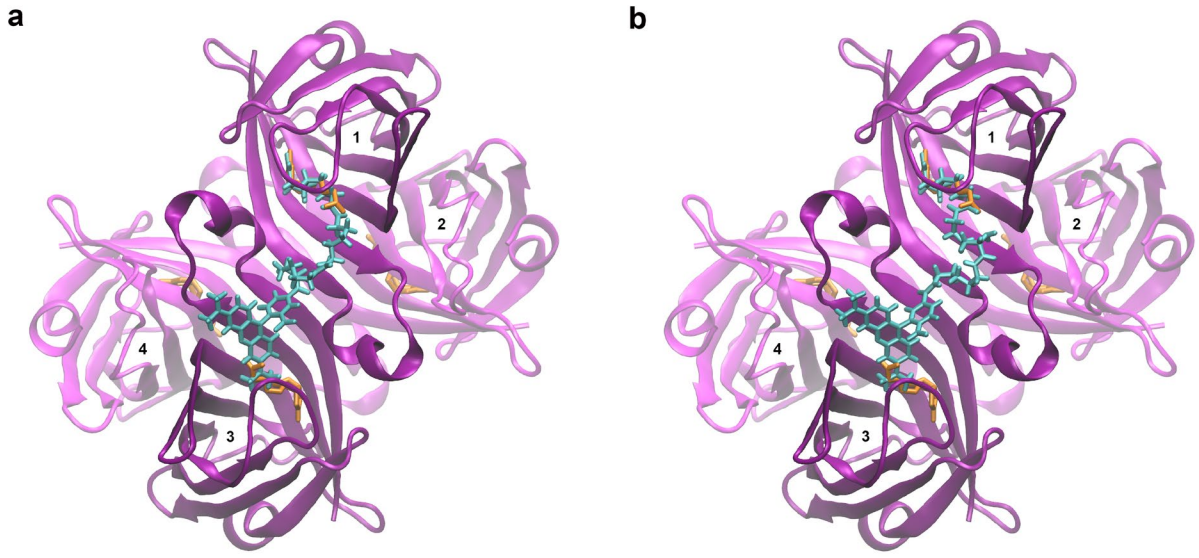

Fig. 2 Docking structure of (a) 5-TMR-biocytin and (b) 6-TMR-biocytin. Biotin binding sites are colored in orange and TMR-biocytin ligands are colored in cyan. Biotin parts of the ligands are bound to monomer 1 and TMR is bound to monomer 3.

Another interesting aspect is that after the biotin part of the ligand is bound to one of the four binding sites (monomer **1** in Fig. 2), TMR can only enter a specific one of the remaining three binding sites (monomer **3** in Fig. 2). Namely, the TMR part of the ligand cannot bind to monomer **2** or **4** if its biotin part is already bound to monomer **1**. This is well illustrated with a simple structural analysis of streptavidin. We found from the structure of streptavidin – biotin complex that the distance between binding sites of monomers **1** and **3** (~20 Å) is much shorter than that between **1** and **2** (~30 Å) and **1** and **3** (~35 Å). Taking all these into account, we can conclude that the fluorescent behavior of TMR is solely due to the interaction between TMR-biocytin and **1**/**3** dimer or **2**/**4** dimer of streptavidin. In this sense, these dimer pairs can be considered as functional dimers in terms of the fluorescence phenomenon, similarly to an earlier report by Lim et al.(Lim, 2011)

For all the simulations after docking, the AMBER03 force field[25] and the general AMBER force field (GAFF)[26-28] were applied to streptavidin and the ligands, respectively. Each complex

of the docked ligand and the protein was placed in a triclinic box of 150 Å × 77.8 Å × 80 Å size and was rotated such that the principal axis of the TMR binding pocket is along the *x*-axis direction. Then, each of the complexes involving biotin, 5-TMR-biocytin, and 6-TMR-biocytin was independently solvated with 28253, 28220, and 28225 TIP3P[29] water molecules. To neutralize each system, 64 Na^+ and 56 Cl^- ions were added. This roughly corresponds to the NaCl concentration of 100 mM. After these constructions, steepest descent minimizations were conducted for each system.

Simulation: free energy calculations

All MD simulations were performed using the GROMACS 5.1.5 package.[30] Short-ranged nonbonded interactions were described using 14 Å cutoff using the Verlet scheme[31] and the long range electrostatics were calculated by the PME algorithm.[32, 33] To account for the truncation of the van der Waals terms caused by the cutoff, dispersion corrections[34] for the pressure and the energy terms were applied. The integration step size was taken to be 2 fs for all simulations. Before the pulling simulation for the free energy calculations, 200 ps NVT and 200 ps NPT equilibrations were performed sequentially with position restraints applied to heavy atoms. All bonds were constrained with the LINCS algorithm[35] in both phases of equilibration. During the NVT equilibration, the ligand-streptavidin complex and its surrounding atoms were separately coupled to heat baths maintained at 300 K. For this, the Berendsen weak coupling method[36] with a relaxation time of 0.1 ps was adopted. For the NPT equilibration, similar weak coupling[36] with a relaxation time of 2 ps was used to maintain the pressure at 1.0 bar, in combination with the same thermalization as in the NVT equilibration.

This was followed by the pulling simulations, namely the production MD. In this case, all bonds involving hydrogen atoms were constrained with the LINCS algorithm. In addition, the

Nose-Hoover thermostat[37, 38] and the Parrinello-Rahman barostat[39] were used to maintain the temperature and the pressure, with a relaxation time of 1 ps for both. The monomer **1** in Fig. 2 was fixed as immobile reference and the ligands were pulled away along the *x*-axis from the monomer **3**, which contains the binding pocket for both TMR and biotin. A spring constant of 1000 kJ/mol·nm^2 and a pulling rate of 0.0125 Å/ps were employed.

To take into account the active site flap[40], the actual binding site, namely monomer **3,** was not restrained for generating proper configurations. Especially for TMR-pulling, the biotin part of the ligand was also fixed to make sure that only TMR was separated from the pocket. The TMR and the biotin pulling simulations were conducted for 2.0 ns and 2.5 ns, respectively.

From the trajectories of the pulling simulations, snapshots were taken to generate the initial configuration of umbrella sampling. The spacing between the umbrella windows were initially taken to be 1 Å along the *x*-component of the center-of-mass separation (ξ), and a few more windows were later added to cover high-energy states. A total of 35 (ξ in 8.0 Å – 40 Å), 28 (ξ in 16 Å – 43 Å), and 31 (ξ in 16 Å – 43 Å) windows were used for biotin, 5-TMR biocytin, and 6-TMR biocytin, respectively. In each window, 100 ps NPT equilibration was first performed using the same method described above. Following the NPT equilibrations, 100 ns MD simulations were performed for the umbrella sampling in each window. During these production simulations, all restraints were removed from the protein and the ligands except from the monomer **1**, which was defined as the immobile reference. The results were analyzed by the weighted histogram analysis method (WHAM)[41] implemented in GROMACS.[42] All structures were visualized by Visual Molecular Dynamics (VMD).[43]

To check if there is any significant structural change in streptavidin caused by TMR-biocytin binding, additional 100 ns of MD simulations of TMR-biocytin – streptavidin systems

were also conducted. Because structural alteration in streptavidin may also cause TMR fluorescence quenching, it will be prudent to check whether any such alteration is actually taking place toward to discovering the underlying physics of streptavidin-induced TMR quenching.

Experiment: time-resolved fluorescence measurement

Fluorescence lifetimes of TMR-biocytin were measured using a home-built confocal fluorescence microscope (Olympus IX-7). To excite the sample, we used a pulsed diode laser (PicoQuant, PDL 800D) with a pulse width of ~100 ps with the peak maximum positioned at 510 nm. The laser beam passed through various mirrors and lenses to the objective lens of a fluorescence microscope, and the sample was excited by the focus of the TIRF objective lens (Zeiss, alpha Plan-Apochromat, Zeiss). The sample was placed on a cover glass for measurement and the fluorescence arising from the sample was collected by the same objective lens and directed to a gallium arsenide photomultiplier tube (Hammatsu, H7422-40) through a 532 nm Raman edge filter (Semrock, FF02-510/10-25) and a 75 μm pinhole. A time-correlated single photon counting (TCSPC) board (PicoQuant Timeharp 260 PICO) was used to record the photon arrival times for the fluorescence decay. Photon arrival times were obtained until enough photons were collected for fluorescence lifetime analyses. The time resolution of this experiment was determined to be ~200 ps based on Raman scattering of water.

The 5-(and-6)-TMR-biocytin and streptavidin were respectively purchased from Thermo Fisher and Agilent, and were used without further purification. Both reagents were dissolved in 10 mM $NaHCO_3$ solution. Glass coverslips for fluorescence lifetime measurements were cleaned with a plasma cleaner (Harrick Plasma, PDC-32G-2) and then coated with a supported lipid bilayer

(POPC) to prevent non-specific adhesion of streptavidin to the cover slip surface.

Results and Discussion

Binding of biotin to streptavidin

To confirm the reliability of our binding free energy calculations, we first obtained the binding affinity of biotin to streptavidin. Fig. 3 shows the free energy profile from the biotin pulling simulations.

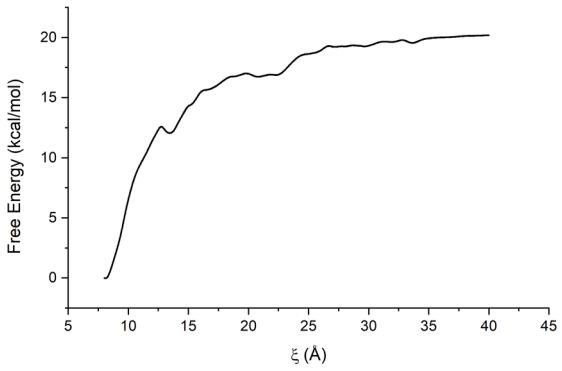

Fig. 3 Free energy profile obtained from the biotin pulling simulations.

To confirm the statistical convergence, we calculated the binding affinities by varying the simulation time of each window from 10 ns to 100 ns. The statistical errors were estimated with the Bayesian bootstrap method[42] (Rubin, 1981) by generating 1000 bootstrap profiles. This method predicts the statistical uncertainty by assigning random weights to the histograms and conducting WHAM using the modified histograms. The validity of the obtained free energy profiles and the standard error values are discussed in Fig. S1. As shown in Fig. S2, the calculated binding free energy converges as the simulation time increases, with the fluctuations becoming negligible compared to the statistical error. The binding affinity of biotin to streptavidin calculated based on Figs. 3 and S2 (ΔG_{BTN}) is -20.2 ± 1.4 kcal/mol, which is in good agreement with the experimental

value of −18.3 kcal/mol.[44] This illustrates that our method is appropriate in estimating the binding free energies of biotin to streptavidin and likely of other biotin-related ligands.

Binding of TMR to streptavidin

Although the adopted docking algorithm may not be perfect in proposing the correct binding site, it is still sufficient toward confirming the weak interaction and finding the possible quenchers of TMR. Starting from the docked structure of 5-(and-6)-TMR-biocytin, we calculated the binding affinity of TMR to streptavidin together with the statistical errors, again by varying the simulation time of each window from 10 ns to 100 ns (Fig. S3). The validity of the obtained free energy profiles and the analysis on the standard error values are discussed in Fig. S. Because the biotin parts of the ligands were fixed during pulling, they were unrealistically stretched after a certain point and displayed unphysical behaviors. This was the reason the free energy of both simulations abruptly increased after certain pulling distances. By analyzing the pulling trajectories and the free energy profile (Fig. 4), we decided that TMR was pulled enough to allow biotin to enter the receptor pocket after ξ = 32.9 Å and ξ = 33.2 Å respectively for complexes with 5-TMR-biocytin and 6-TMR-biocytin. These values were chosen based on two criteria; (1) biotin could enter the binding pocket with a center-of-mass spacing larger than these values and (2) the center-of-mass pulling energies plateaued at least momentarily beyond the distances except for some small fluctuations near zero (Fig. S5).

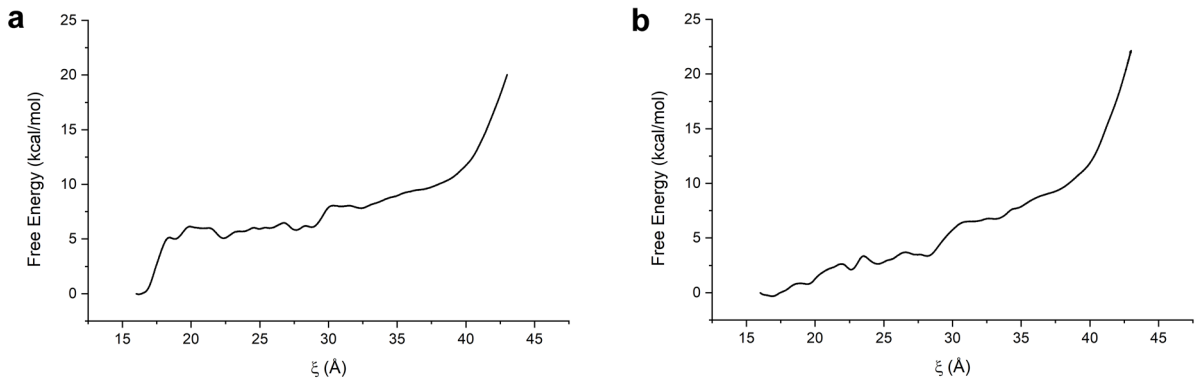

Fig. 4 Free energy profiles from the pulling simulations with (a) 5-TMR-biocytin and (b) 6-TMR-biocytin.

To streptavidin, the calculated binding affinities of the TMR moieties in 5-TMR-biocytin and 6-TMR-biocytin are respectively $\Delta G_{5\text{-TMR}} = -8.06 \pm 0.79$ kcal/mol and $\Delta G_{6\text{-TMR}} = -6.91 \pm 0.72$ kcal/mol. Indeed, both of these values are much smaller than the biotin binding affinity, which reflects the fact that biotin binds much more strongly to streptavidin than TMR does. Interestingly, these values are in close agreement with the binding free energy of anionic 1-anilino-8-naphthalene sulfonate to bovine serum albumin (BSA) observed with calorimetry titration (within −6 to −7 kcal/mol at pH 2.0). In any case, based on the binding affinity values, we could obtain ΔG of the process where biotin frees up TMR units from streptavidin. Let us suppose the following reactions that causes the fluorescence quenching and recovery of TMR:

$$T_5 + S \rightleftharpoons S^{+T_5} \quad (1)$$

$$T_6 + S \rightleftharpoons S^{+T_6} \quad (2)$$

$$S^{+T_5} + S^{+T_6} + 2B \rightleftharpoons BS^{-T_5} + BS^{-T_6} \quad (3)$$

The steps (1) and (2) represent the binding between the 5-(and-6)-TMR-biocytin and streptavidin. When biotin is added to the bound complexes, it frees up the TMR units but the TMR-biocytin

species are still bound to streptavidin through the biocytin moiety. This is represented by the step (3). The free energy of this last step can be obtained as

$$\Delta G = 2\Delta G_{\mathrm{BTN}} - (\Delta G_{5\text{-TMR}} + \Delta G_{6\text{-TMR}})$$

The calculated ΔG of this replacement reaction is -25.4 ± 3.0 kcal/mol.

Osborne actually estimated the interaction energy between TMR and streptavidin by calculating the electrostatic potential between charged amino acid residues on the protein surface and zwitterionic TMR.[16] His calculations actually suggested an upper bound of the binding energy as about −14 kcal/mol. In the sense that this value is an upper bound, his estimation is in an agreement with our results of $\Delta G_{5\text{-TMR}}$ and $\Delta G_{6\text{-TMR}}$. The reason the upper bound value is almost twice larger than our estimation can be ascribed to the fact that his calculations were based on rather simple assumptions of considering only oppositely charged nearest-neighbor pairs between streptavidin and TMR without taking into account the interaction between the linker part of TMR and the protein. In addition, the effect of solvent was estimated implicitly. Of course, fluctuating ensemble (entropy) was not considered either as in our free energy calculations.

Fluorescence quenching and TMR-streptavidin weak interaction

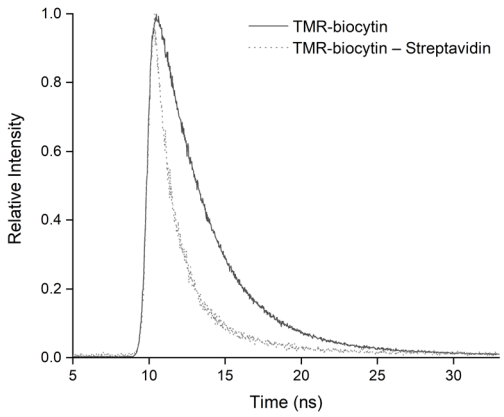

Fig. 5 Time-resolved fluorescence decays of 200 nM TMR-biocytin with and without streptavidin. The solid curve is obtained in the absence of added streptavidin, while the dotted line has excess streptavidin. The excitation wavelength was λ_{ex} = ~510 nm and TCSPC was obtained by collecting with λ_{em} > 532 nm. When enough biotin was added to the TMR-biocytin – streptavidin complex, the fluorescence decay pattern was practically identical to the case of free TMR-biocytin.

Table 1. Exponential fitting results of TCSPC data.[a]

	A_1	τ_1 (ns)	A_2	τ_2 (ns)	τ_{avg} (ns)[b]
TMR-biocytin	-	3.36	-	-	3.36
TMR-biocytin – streptavidin	0.389	3.2	1.07	1.17	2.50

[a] The fluorescence decay curves in Fig. 5 were fit by $f(t) = A_1 e^{-t/\tau_1} + A_2 e^{-t/\tau_2}$. [b] Weighted average given by $\tau_{avg} = (A_1\tau_1 + A_2\tau_2) / (A_1 + A_2)$.

Figure 5 shows the time-resolved fluorescence decays of TMR-biocytin in the absence and the presence of excess streptavidin. The samples were excited with a 510 nm diode laser and the fluorescence was collected using a 532 nm dichroic mirror and Raman edge. In order to minimize the binding of two or more TMR-biocytin to a single streptavidin, excess streptavidin was added to TMR-biocytin (100-fold). With bi-exponential fitting of the data, the fluorescence

lifetime of free TMR-biocytin was obtained as 3.54 ns. With streptavidin binding, it decreases to 2.54 ns (Table 1). The decrease in fluorescence lifetime reflects that the fluorescence of TMR-biocytin was quenched by streptavidin. Fig. 5 also shows that when a sufficient amount of biotin is added to TMR-biocytin – streptavidin complex, the fluorescence lifetime was completely recovered.

Because fluorescence is sensitive to the local environment, it can indeed provide useful information about the surroundings of macromolecules, such as the distance between two specific sites. The two main mechanisms that cause fluorescence change are Förster resonance energy transfer (FRET) and photoinduced electron transfer (PET). One may be concerned that the structure alteration induced by TMR-biocytin binding can also cause the fluorescence quenching, but the 100 ns MD simulations of TMR-biocytin – streptavidin system did not show any significant structural change on the protein. Namely, as shown in Fig. 6, the root mean square deviation (RMSD) values during the simulations converged to less than 3 Å, affirming that the structure alteration of streptavidin will not be a direct cause of TMR fluorescence quenching.

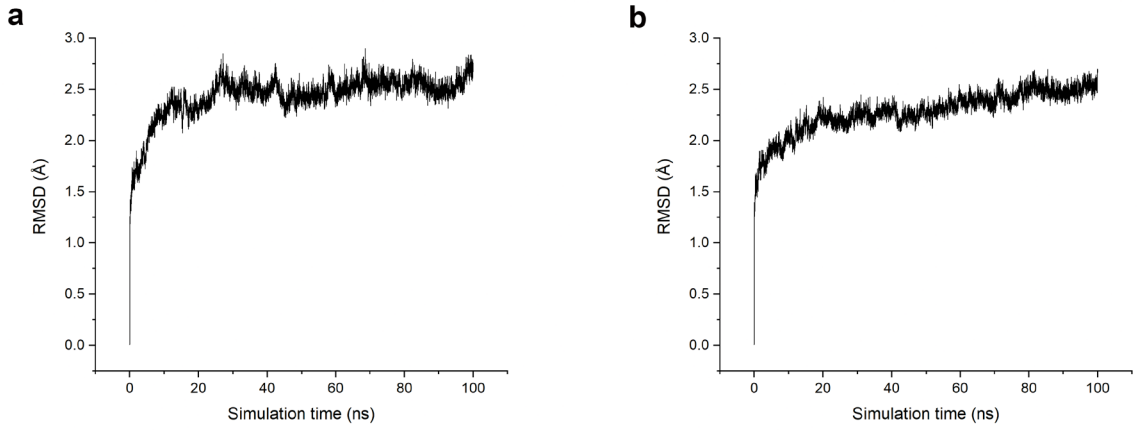

Fig. 6 Change in RMSD of streptavidin upon ligand binding with (a) 5-TMR-biocytin and (b) 6-TMR-biocytin. The protein structure at $t = 0$ was taken as the reference structure for calculating RMSD values.

The FRET efficiency relies on the distance between the energy donor and the energy acceptor (typically 1 – 10 nm), whereas PET occurs well when the distance between the electron donor and the electron acceptor is within 1 nm.[45] Tryptophan is well known for its quenching capability. Namely, it behaves as an efficient electron donor in the photoinduced electron transfer (PET)[46, 47] and causes quenching of TMR within sub-nanometer spacing.[48, 49]

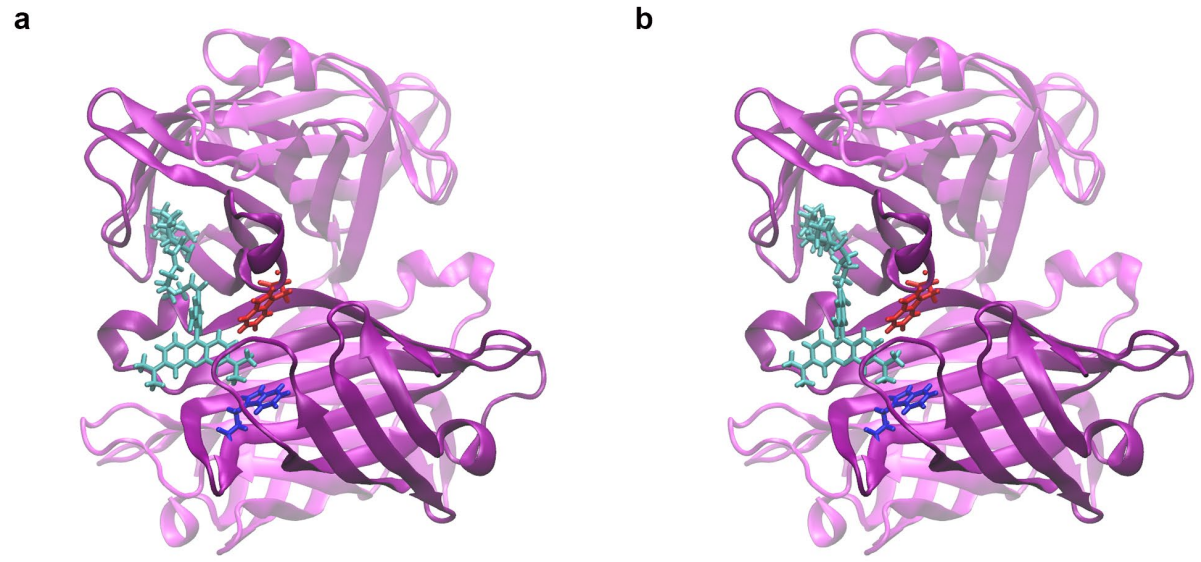

Fig. 7 Two tryptophan residues closest to the TMR portion of (a) 5-TMR-biocytin and (b) 6-TMR-biocytin, complexed with streptavidin. TRP79 is colored in blue and TRP120 is colored in red.

As stated in a previous section, our calculations imply that a weak interaction actually exists between TMR and streptavidin, specifically around the entrance portal of the binding pocket (Fig. 2). This is again presented in Fig. 7, where we are additionally showing the locations of nearby tryptophan residues. Because biotin interacts with streptavidin significantly stronger than TMR does, biotin can occupy nearly all of the receptor pockets of streptavidin when both TMR-biocytin and biotin are present in the system. Furthermore, the fact that the calculated ΔG is negative (namely, the forward reaction is favored) is in good agreement with the experimental result that the fluorescence of TMR is recovered after biotin is added to the system. This shows

that the relative binding energies derived from docking is quite reliable, and likely the docking-suggested structure is reliable. Based on this suggested structure, we can propose a plausible mechanism of TMR fluorescence quenching and recovery induced by streptavidin binding at a molecular level in relation to the locations of potentially quenching tryptophan residues. Indeed, Fig. 7 shows how TMR and tryptophan residues are spatially aligned when TMR binds to the entrance of the binding pocket. Namely, they are quite close in space and quenching by tryptophan residues are quite plausible and the TMR-pocket interaction is not likely the quencher. For the docked structure of 6-TMR-biocytin, the center-of-mass distances between the core xanthene group of TMR and indole parts of the two closest tryptophan residues (TRP79, TRP120) are 9.02 Å and 8.84 Å, respectively. With 5-TMR-biocytin, the closest distances are 8.91 Å and 9.04 Å. Thus, the fluorescing TMR "head" does not have to be hidden in the pocket as the ostrich model literally suggests.

In fact, there have been repeated reports on the photoinduced electron transfer between fluorescent materials and tryptophan. Smith and coworkers investigated the fluorescence quenching of rhodamine 6G (R6G) by tryptophan in aqueous solution using fluorescence spectroscopy and MD simulations.[49] Their results revealed that PET occured within 10 Å between R6G and tryptophan. Therefore, the sub-nanometer spacings between TMR and tryptophan residues found in our structures will be small enough to promote fluorescence quenching of TMR-biocytin.

In addition, it is important to compare the different quenching behaviors when streptavidin is free in solution or is surface-attached. The site where TMR binds to streptavidin is solvent-accessible, whereas the same site becomes inaccessible when streptavidin is attached to a surface because the surface blocks pocket opening.[16] This is consistent with a report by Osborne that the

fluorescence quenching of TMR-biocytin was rarely observed at the single molecule level when surface-attached streptavidin was employed to consume TMR-biocytin.

The binding energy of TMR and streptavidin calculated in this study may play a guiding role in studying fluorescence changes arising from the interaction between other fluorophores and proteins. The previously reported fluorescence quenching of fluorescein-biotin conjugate by streptavidin can also be explained in a similar manner as described in this paper. We also expect that the present study can be extended to understanding the well-known 4'-hydroxyazobenzene-2-carboxylic acid (HABA) dye-streptavidin system.

Conclusions

In this work, we obtained the possible binding site of biotinylated TMR to streptavidin that could explain the "ostrich quenching" of biotinylated dyes. All the docking structures of TMR-biocytin to streptavidin proposed by Autodock Vina showed enough consistency to confirm its interaction with protein that leads to TMR fluorescence quenching. We applied the umbrella sampling method to the system to calculate the binding affinity of TMR, which indeed confirmed that the interaction between TMR and streptavidin does actually exist and it is much weaker than that of biotin (−8.06 kcal/mol for 5-TMR-biocytin and −6.91 kcal/mol for 6-TMR-biocytin). When we applied the same protocol to biotin-streptavidin system, we obtained the biotin binding affinity of −20.2 kcal/mol, which was in a very good agreement with the experimental value of −18.3 kcal/mol. This agreement indeed validates our umbrella sampling strategy over the rather complicated complex structures. The binding affinity values suggest that there actually exists a weak interaction between TMR and streptavidin. We also employed time-resolved fluorescence to observe the fluorescence quenching and recovery of TMR in the system composed of streptavidin,

biotin, and TMR-biocytin. The fluorescence lifetime of TMR-biocytin decreased from 3.54 ns to 2.54 ns in the presence of excess streptavidin. To elucidate the origin of the fluorescence quenching/recovery of TMR, we further analyzed the binding site of TMR based on the conformations obtained from our simulations. We found that TMR did not bind perfectly to the biotin binding pocket, but it only bound to the entrance of the pocket. Thus, the interaction with the pocket should not be the direct cause of the fluorescence quenching. In addition, streptavidin did not display any meaningful structural change upon the ligand binding. Based on these aspects, we suggested that the fluorescence quenching was caused by the tryptophan residues of streptavidin in close proximity with the dye unit.

In summary, we investigated the interaction between TMR and streptavidin and analyzed their weak interaction, which can drive the interesting fluorescence modulation. It is intriguing that we could provide new information regarding the streptavidin-biotin interaction and the related fluorescence quenching of biotinylated dye by streptavidin binding, although the phenomenology has long been known to scientists. This was possible with the details at the molecular level that were reached from the theory side, which showed that there actually exists a weak interaction between TMR itself and streptavidin as well as biotin and streptavidin. In addition, we presented that TMR cannot bind to the receptor pocket as perfectly as biotin and it rather blocks the entrance portal of the biotin binding pocket. We hope that the present study can allow us to understand the TMR-streptavidin interactions better and also to help developing tools that can be generally applied for studying other CPIs.

Acknowledgements

This work was supported by National Research Foundation (NRF) of Korea (No.

2020R1A5A1019141) funded by the Ministry of Science and ICT (MSIT).

References

1. S. I. Park, J. Shenoi, S. M. Frayo, D. K. Hamlin, Y. K. Lin, D. S. Wilbur, P. S. Stayton, N. Orgun, M. Hylarides, F. Buchegger, A. L. Kenoyer, A. Axtman, A. K. Gopal, D. J. Green, J. M. Pagel and O. W. Press, *Clin. Cancer Res.*, 2011, **17**, 7373-7382.
2. K. Fletcher and N. B. Myant, *Nature*, 1960, **188**, 585.
3. R. J. McMahon, *Annu. Rev. Nutr.*, 2002, **22**, 221-239.
4. E. Livaniou, D. Costopoulou, I. Vassiliadou, L. Leondiadis, J. O. Nyalala, D. S. Ithakissios and G. P. Evangelatos, *J. Chromatogr. A*, 2000, **881**, 331-343.
5. M. Tanaka, Y. Izumi and H. Yamada, *J. Microbiol. Methods*, 1987, **6**, 237-246.
6. P. Vilja, L. Wichmann, T. Visakorpi, K. Krohn and P. Tuohimaa, *Scand. J. Immunol.*, 1986, **24**, 482-482.
7. Y. Wu, P. C. Simons, G. P. Lopez, L. A. Sklar and T. Buranda, *Anal. Biochem.*, 2005, **342**, 221-228.
8. C. T. Lin, M. T. Kao, K. Kurabayashi and E. Meyhofer, *Nano Lett.*, 2008, **8**, 1041-1046.
9. L. Cognet, G. S. Harms, G. A. Blab, P. H. M. Lommerse and T. Schmidt, *Appl. Phys. Lett.*, 2000, **77**, 4052-4054.
10. H. J. Gruber, M. Marek, H. Schindler and K. Kaiser, *Bioconjugate Chem.*, 1997, **8**, 552-559.
11. T. Buranda, G. P. Lopez, P. Simons, A. Pastuszyn and L. A. Sklar, *Anal. Biochem.*, 2001, **298**, 151-162.
12. P. C. Simons, M. Shi, T. Foutz, D. F. Cimino, J. Lewis, T. Buranda, W. K. Lim, R. R.

Neubig, W. E. Mcintire, J. Garrison, E. Prossnitz and L. A. Sklar, *Mol. Pharmacol.*, 2003, **64**, 1227-1238.

13. T. Buranda, J. M. Huang, V. H. Perez-Luna, B. Schreyer, L. A. Sklar and G. P. Lopez, *Anal. Chem.*, 2002, **74**, 1149-1156.

14. W. C. Jackson, F. Kuckuck, B. S. Edwards, A. Mammoli, C. M. Gallegos, G. P. Lopez, T. Buranda and L. A. Sklar, *Cytometry*, 2002, **47**, 183-191.

15. T. Buranda, G. M. Jones, J. P. Nolan, J. Keij, G. P. Lopez and L. A. Sklar, *J. Phys. Chem. B*, 1999, **103**, 3399-3410.

16. M. A. Osborne, *J. Phys. Chem. B*, 2005, **109**, 18153-18161.

17. G. N. Patey and J. P. Valleau, *Chem. Phys. Lett.*, 1973, **21**, 297-300.

18. G. M. Torrie and J. P. Valleau, *Chem. Phys. Lett.*, 1974, **28**, 578-581.

19. G. M. Torrie and J. P. Valleau, *J. Comput. Phys.*, 1977, **23**, 187-199.

20. P. C. Weber, D. H. Ohlendorf, J. J. Wendoloski and F. R. Salemme, *Science*, 1989, **243**, 85-88.

21. M. D. Hanwell, D. E. Curtis, D. C. Lonie, T. Vandermeersch, E. Zurek and G. R. Hutchison, *J. Cheminform.*, 2012, **4**, 17.

22. G. M. Morris, R. Huey, W. Lindstrom, M. F. Sanner, R. K. Belew, D. S. Goodsell and A. J. Olson, *J. Comput. Chem.*, 2009, **30**, 2785-2791.

23. A. K. Rappe, C. J. Casewit, K. S. Colwell, W. A. Goddard and W. M. Skiff, *J. Am. Chem. Soc.*, 1992, **114**, 10024-10035.

24. O. Trott and A. J. Olson, *J. Comput. Chem.*, 2010, **31**, 455-461.

25. Y. Duan, C. Wu, S. Chowdhury, M. C. Lee, G. Xiong, W. Zhang, R. Yang, P. Cieplak, R. Luo, T. Lee, J. Caldwell, J. Wang and P. Kollman, *J. Comput. Chem.*, 2003, **24**, 1999-2012.

26. J. Wang, R. M. Wolf, J. W. Caldwell, P. A. Kollman and D. A. Case, *J. Comput. Chem.*, 2004, **25**, 1157-1174.

27. J. Wang, W. Wang, P. A. Kollman and D. A. Case, *J. Mol. Graph. Model.*, 2006, **25**, 247-260.

28. A. W. Sousa da Silva and W. F. Vranken, *BMC Res. Notes*, 2012, **5**, 367.

29. W. L. Jorgensen, J. Chandrasekhar, J. D. Madura, R. W. Impey and M. L. Klein, *J. Chem. Phys.*, 1983, **79**, 926-935.

30. M. J. Abraham, T. Murtola, R. Schulz, S. Páll, J. C. Smith, B. Hess and E. Lindahl, *SoftwareX*, 2015, **1-2**, 19-25.

31. S. Pall and B. Hess, *Comput. Phys. Commun.*, 2013, **184**, 2641-2650.

32. T. Darden, D. York and L. Pedersen, *J. Chem. Phys.*, 1993, **98**, 10089-10092.

33. U. Essmann, L. Perera, M. L. Berkowitz, T. Darden, H. Lee and L. G. Pedersen, *J. Chem. Phys.*, 1995, **103**, 8577-8593.

34. E. Lindahl, M. J. Abraham, B. Hess and D. Van der Spoel, GROMACS Documentation, https://zenodo.org/record/3562512#.YD3vqugzZbB, (accessed March 2021, DOI: https://doi.org/10.5281/zenodo.3562512).

35. B. Hess, H. Bekker, H. J. C. Berendsen and J. G. E. M. Fraaije, *J. Comput. Chem.*, 1997, **18**, 1463-1472.

36. H. J. C. Berendsen, J. P. M. Postma, W. F. Vangunsteren, A. Dinola and J. R. Haak, *J. Chem. Phys.*, 1984, **81**, 3684-3690.

37. S. Nose, *Mol. Phys.*, 1984, **52**, 255-268.

38. W. G. Hoover, *Phys. Rev. A*, 1985, **31**, 1695-1697.

39. M. Parrinello and A. Rahman, *J. Appl. Phys.*, 1981, **52**, 7182-7190.

40. N. Bansal, Z. Zheng, L. F. Song, J. Pei and K. M. Merz, Jr., *J. Am. Chem. Soc.*, 2018, **140**, 5434-5446.

41. S. Kumar, D. Bouzida, R. H. Swendsen, P. A. Kollman and J. M. Rosenberg, *J. Comput. Chem.*, 1992, **13**, 1011-1021.

42. J. S. Hub, B. L. de Groot and D. van der Spoel, *J. Chem. Theory Comput.*, 2010, **6**, 3713-3720.

43. W. Humphrey, A. Dalke and K. Schulten, *J. Mol. Graph. Model.*, 1996, **14**, 33-38.

44. A. Chilkoti and P. S. Stayton, *J. Am. Chem. Soc.*, 1995, **117**, 10622-10628.

45. S. Doose, H. Neuweiler and M. Sauer, *ChemPhysChem*, 2009, **10**, 1389-1398.

46. M. Rebarz, J. Ghesquiere, A. Boisdenghien, E. Defrancq, C. Moucheron and A. Kirsch-De Mesmaeker, *Inorg. Chem.*, 2010, **49**, 10867-10874.

47. D. S. Wilbur, P. M. Pathare, D. K. Hamlin, M. B. Frownfelter, B. B. Kegley, W. Y. Leung and K. R. Gee, *Bioconjugate Chem.*, 2000, **11**, 584-598.

48. N. Marme, J. P. Knemeyer, M. Sauer and J. Wolfrum, *Bioconjugate Chem.*, 2003, **14**, 1133-1139.

49. A. C. Vaiana, H. Neuweiler, A. Schulz, J. Wolfrum, M. Sauer and J. C. Smith, *J. Am. Chem. Soc.*, 2003, **125**, 14564-14572.